ACS OMEGA

http://pubs.acs.org/journal/acsodf

Article

Contactless Method for Electrocoalescence of Water in Oil

Mohcen Shahbaznezhad, Amir Dehghanghadikolaei, and Hossein Sojoudi*

Cite This: *ACS Omega* 2021, 6, 14298−14308

Read Online

ACCESS | Metrics & More | Article Recommendations | Supporting Information

ABSTRACT: This paper discusses an experimental approach to study the effects of a contactless method on electrocoalescence of water-in-oil mixture/emulsion. A positive corona discharge is utilized using a sharp conductive needle without direct contact with the mixture/solution to avoid potential corrosion of the electrode. This creates a nonuniform electric field, which is further used for the coalescence of water droplets in the range of micro to macro in oil. Two approaches are employed in this study: qualitative analysis conducted by visually studying coalescence patterns in videos captured with a high-speed camera and a quantitative analysis based on calculations obtained from dynamic light scattering measurements. From the behavior of the water droplets under the electric field, it is observed that dipole−dipole interaction, migratory coalescence/electrophoresis, and dielectrophoresis have major roles in promoting the coalescence events. The effects of oil viscosity and power consumption on the coalescence rate are also investigated, suggesting an optimal oil−water separation process. The results of this study pave a path for developing a safe, contactless, rapid, and low-power-consuming separation process, potentially suitable for an offsite application.

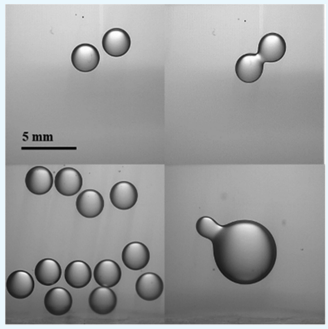

1. INTRODUCTION

1.1. Separation of Water from Oil. The separation of water from an emulsion is the most common processing step in applications such as petroleum de-emulsification, chemical dehydration, desalination, wastewater treatment processes, and other industries such as resource recycling, metallurgy, and equipment manufacturing.[1,2] Water and oil mixtures can be separated by exerting external forces, self-induction, gravity forces, and buoyancy forces enabling their separation and removal.[3,4] In gravity separator setups, the sedimentation time of the small water droplets (sizes less than 100 μm) is in close correlation with the residence velocity.[5] The sedimentation time for water droplets significantly changes with their size, and it can vary from seconds to years for sizes ranging from macro- to microscale.[6] The motion of water droplets toward each other triggered via mechanical forces,[7] microwave radiation,[8] thermal forces,[9] electrostatic forces,[10] membrane separation,[11] demulsifier,[12] adsorption,[13] absorption,[14] and chemical reactions[15] governs the separation rate in the emulsion. However, electrocoalescence is the most common method of coalescence used in various industries, providing a fast and efficient separation of emulsions.[1]

1.2. Electrocoalescence. The separation of a water droplet induced by external electric fields results in the generation of a dipole that further interacts with another adjacent dipolar water droplet, enhancing the coalescence rate in an emulsion. This process is called dipole−dipole interaction (DDI), which is considered the primary mechanism for observing electrocoalescence in a uniform electric field. The motion of water droplets can also be induced via Coulombic forces caused by an external electric field on charged water droplets, enhancing the chances of collision between the water droplets and leading to the so-called migratory coalescence. The migratory coalescence is mainly due to the electrophoresis (EP) force and is observed when utilizing DC electric fields; a few studies available in the literature investigated this effect on the electrocoalescence process. Overall, the kinetics of electrocoalescence events are governed by various parameters such as electrical and physical properties of the fluids, the magnitude of the external electric fields, emulsion impurities, flow and turbulence of the fluids, water droplet sizes, and dispersion of water droplets, which have been extensively investigated in the literature.[16−19] However, chain formation, water droplet splitting, low performance on the low water content, residue water droplets, and high-power consumption, particularly for AC electric field, are some of the incidents that have adverse effects on the electrocoalescence rates and performances. These incidents could potentially occur due to the application of moderate electric fields during separation processes.[3] For instance, alignment of the water droplets in the direction of the applied electric field forms a water bridge in the shape of a chain that causes an electric discharge (i.e., short circuit) and consequently a reduced coalescence rate.[20,21] These adverse characteristics can be alleviated either by coating the electrode tip with thin layers of dielectric materials with a compromise of extra cost and additional required electric field/power consumption. Alternatively, using a

Received: February 26, 2021
Accepted: May 14, 2021
Published: May 28, 2021

microfluidics setup could eliminate the chances of chain formation by continuous motion of the fluid inside the channels. However, the scalability of the microfluidic channels/devices is limited and they are not suitable for offsite industrial applications.[22] Also, electrode corrosion is another challenge due to the electrolytic effect at anode electrodes (especially when utilizing DC electric fields).[23]

In general, changing the strength of the electric field leads to 2 orders of magnitude enhancement in the coalescence rate of water droplets.[24] Some studies have shown that there is an electric field threshold in emulsions below which electrocoalescence cannot be fully triggered, requiring the intensity of the electric field to be increased to activate DDI and EP.[25] Furthermore, improving the performance of these two mechanisms is corresponded to increasing the strength of the electric field. However, by increasing the field strength, it is most likely to form water droplet chains across the electrodes and split water droplets undesired in the coalescence process. Williams suggested three electrostatic splitting mechanisms. Water droplets will be elongated along the direction of the electric field and will be disintegrated if the electric field is strong enough. Another mechanism related to constraining the acquired charges by coming into contact with the electrode or charged water droplets is given by Rayleigh. The third disintegration mechanism is triggered when the water droplets are attached to one of the electrodes. In this case, charges accumulate at the tip of droplets and start forming the Taylor cone, which produces small droplets at the tip of the water droplet (shown in Video S1).[26,27] This issue could be mitigated by applying a hydrophobic coating to the electrode to prevent droplet formation on the electrode; however, it requires extra cost. In spite of increasing the strength of the electric field, in some cases, the water droplets retreat after initial contact with each other forming noncoalescence water droplets; thus, this increase in an electric field can decrease the efficiency of the coalescence and ultimately the separation process.[28,29] To avoid activating those mechanisms and increasing the interaction force (coalescence rate), it is needed to determine a general strategy to solve this problem. Recent studies have shown promising results by utilizing nonuniform electric fields for emulsion separation with improvement in the dehydration process and accelerating the movement of water droplets.[30,31] However, an optimum electrode geometry for creating a nonuniform electric field remains challenging, mostly due to the Joule heating effect.[24,32,33] To address this challenge, it is required to have a flexible and contactless method when applying electric discharge and forming nonuniform electric fields.

1.3. Corona Discharge. Corona discharge provides many advantages in several industrial applications such as photocopying, ozone generating, and air filtration.[34] When a neutral gas (i.e., air) is introduced into a high potential gradient, it results in gas ionization and loss of neutrality. The most common configuration to create corona discharge is a point-to-plane setup. The gas in the space near the sharp conductive electrode ionizes when a threshold voltage is applied, sustaining a continuous discharge regime. In a positive corona discharge, positive ions of gaseous medium form free space charge carriers accelerating toward the negative ground electrode.[35,36]

Here, a contactless method of emulsion separation is presented utilizing a nonuniform electric field induced via a corona discharge. The corona discharge generates ions for inducing an electrohydrodynamic (EHD) instability inside a W/O mixture/emulsion. The charged ions accelerate and drift toward the opposite electrode, creating an ionic wind. Locating the W/O mixture/emulsion between the corona-producing electrode and the ground electrode results in the injection of the ions and the formation of a nonuniform electric field in the mixture/emulsion. Due to the contactless nature of our method, there is no electrode corrosion as a result of exposure to the W/O mixture/emulsion. The air gap between the corona-producing electrode (a sharp conductive needle connected to a high voltage) and the W/O mixture/emulsion acts as a current barrier and results in improving the safety of this separation process. Besides, the nonuniform electric field generated in this configuration eliminates the complexity involved in conventional methods such as the design of the electrode geometry and/or temperature increase due to the Joule heating effect.[33] Finally, the formation of the ionic wind and its injection into the W/O mixture/emulsion induces electroconvection in it, breaking up chain formation by water droplets, which is problematic in conventional electrocoalescence.

2. RESULTS AND DISCUSSION

The corona discharge current/voltage characteristics follow the Townsend discharge regime defined by[37]

$$\frac{I}{V} = k(V - V_0) \tag{1}$$

where I is the current, V is the applied voltage, k is a constant, and V_0 is the corona onset voltage. Indeed, the space charge between the sharp electrode and the liquid surface acts as a large nonlinear resistor or, in other words, acts as current overload protection, playing a safeguard role against short-circuit events. The power loss due to this resistance behavior is trivial (on the order of mW) due to the microamp range of the current. The optimum distance of the electrode (corona gap) on the dielectric liquid was reported in our previous work.[36] Air molecules/atoms were ionized in the area close to the sharp electrode with a high potential gradient. The liberated electrons move toward the sharp electrode, and the positive ions are subjected to an electric field, accelerating from the pointed electrode to the ground electrode. The dielectric liquid can be considered ohmic fluid if the traveling time of the injected ions is less than the relaxation time of the liquid. Otherwise, it is fair to be assumed as a nonohmic fluid[38]

$$\frac{\varepsilon_c \varepsilon_0}{\sigma} > \frac{L^2}{K_L V_L} \tag{2}$$

where ε_c is the dielectric constant of the liquid, ε_0 is the permittivity of free space, σ is the conductivity, L is the thickness, K_L is the ion mobility, and V_L is the surface potential. In this experiment, the relaxation time of silicone oil is calculated to be 400 s (with $\varepsilon = \varepsilon_0 \varepsilon_c$, $\varepsilon_0 = 8.85 \times 10^{-12}$ F/m, $\varepsilon_c = 2.75$, and $\sigma = 6 \times 10^{-12}$ S). On the other hand, the mobility of the ions of the air is much higher than that of liquid mobility and results in charges being trapped on the liquid surface. This situation is called space charge limited current (SCLC); therefore, we can conclude that the silicone oil in our experiments acted as a nonohmic fluid. The electric field in the corona gap can be found by[39]

https://doi.org/10.1021/acsomega.1c01072
ACS Omega 2021, 6, 14298−14308

$$E(x) = \frac{V}{(x + r) \times \ln\left(\frac{2t + r}{r}\right)} \quad (3)$$

where r is the sharp electrode radius of curvature, t is the corona gap, and x is the abscissa of the point to a sharp electrode. The current density in the air is $j = K_a E_q (dE/dz = q/\varepsilon_0)$ and in the liquid is $j = K_L E_q$. From the continuity of εE on the oil surface and by the integration of $V = E \cdot dL$, we can reach the voltage distribution on the oil surface. The surface potential can be found by[40]

$$V = \left(\frac{8J}{9K_L \varepsilon L^2}\right) \quad (4)$$

Utilizing the corona discharge, the ionic wind collides with the W/O mixture/emulsion surface and the current density varies from point to point, which can be found in Warburg's law[41]

$$j = \frac{I_c}{2t^2}(\cos(\alpha))^n \begin{cases} n = 4.82 \text{positive corona} \\ n = 4.65 \text{negative corona} \\ \alpha \leq 65^\circ \end{cases} \quad (5)$$

where I_c is the corona current, α is the angle between the needle and a point on the surface (Figure 1), and n is a constant depending on the positive or negative corona. It can be seen from the above correlation that the current density is concentrated at the centerline aligned with the needle ($\alpha = 0^\circ$) and reaches zero on the sides of the test cell ($\alpha \geq 65^\circ$). The oil surface acts as an electrode in which the surface voltage is distributed as a function of distance to the sharp electrode. This nonuniform distribution of the surface potential and the constant potential of the ground electrode builds a nonuniform electric field in the oil medium ($E = V/L$).[42]

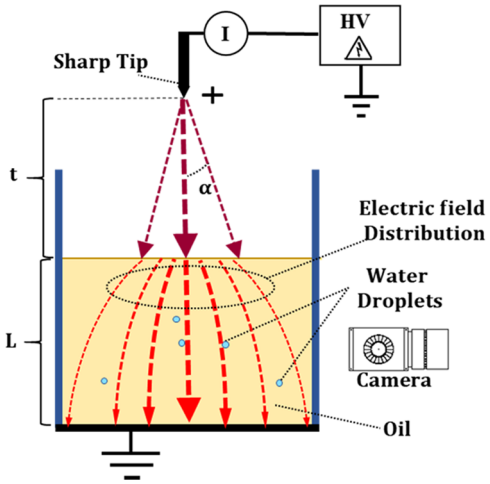

Figure 1. Schematic of the experimental setup. The height of the needle was adjusted by a laboratory jack to which the test cell was fixed. High-voltage potential (V) creates a strong potential gradient between the electrodes resulting in ionization of the air molecules. The charged ions accelerate and drift toward the opposite electrode, creating an ionic wind. When the ionic wind collides with the emulsion surface, the charges are transformed via conduction or convection, making a nonuniform electric field in the dielectric medium. The current density distributes nonuniformly on the W/O mixture/emulsion surface following Warburg's law, presented in eq 5. The electric field is stronger in the center and surface of the W/O mixture/emulsion as a direct result of the current density distribution. Current and voltage were measured actively during the experiments, and videos were captured from the side view of the test cell.

2.1. Coalescence of Two Water Droplets in an Oil Medium. To examine the impact of corona discharge and various electrocoalescence phenomena involved in the process, simple tests were conducted by placing water droplets inside a silicone oil medium, and their trajectories were examined via high-speed imaging. To this end, a table setup was designed to expose water droplets dispersed inside a dielectric oil to corona discharge. Figure 1 shows the schematic of the setup, including mainly three parts: a high-voltage amplifier connected to a sharp electrode for corona generation, an adjustable mechanism used to keep a grounding electrode in contact with the emulsion, and a measuring unit incorporating current measurements (see also Figure S1). First, the test cell was prepared by filling a quartz cube up to 15 mm high with silicone oil of 3000 cSt viscosity, and the corona gap was kept at 10 mm (t = 10 mm). The high viscosity oil was used to increase the sedimentation time of the water droplets to provide enough time to observe the droplets' behaviors during the experiment. The sedimentation velocity is defined by[6]

$$v = \frac{(2a^2(\rho_W - \rho_C)g)}{9\eta} \quad (6)$$

where a is the droplet radius, ρ_W is the droplet (water) density, ρ_C is the continuous phase (oil) density, η is the fluid dynamic viscosity, and g is the gravitational constant.

Four major positions of the water droplets were considered in this experiment to investigate the effect of the DDI, EP, and DEP. The corona voltage was kept constant at 4 kV. This voltage was selected to eliminate the impact of flow motion induced by electroconvection.[43]

The first two water droplets were dispersed closely in the center of the test cell (Figure 2A). In this situation, it was expected that two water droplets form dipoles due to the polarization in the electric field and interact with each other. The distance between the two dipoles was close enough to build large interaction energy and to develop radial and tangential forces, as shown schematically in Figure S2 and described by eqs S1 and S2.[44]

It can be inferred from eqs S1 and S2 that the interaction between two water droplets is significantly affected by their distance (proportional to the inverse of the fourth power of their distance). In addition, an increase in the size of water droplets can enhance coalescer performance by 3-folds. At the beginning of the test, the effect of the radial force was not considerable because of the angle between the dipoles and the distance vector, as can be seen in eq S1; hence, the droplets did not move toward each other. However, the net tangential force was not zero appearing right after polarization based on eq S2. Subsequently, the two dipoles rotated counterclockwise to approach the position where the radial force was high enough to overcome hydrodynamic forces, starting to maneuver. Consequently, the water droplets started to move toward each other and finally coalesced. The entire process occurred in less than 15 s, suggesting the fast response of the DDI mechanism if all of the requirements are met (see Video S2). Figure 2A shows the snapshots of droplets during this coalescence process.

Next, two water droplets were dispersed in the center of the oil medium along the corona tip, and each was touching the

https://doi.org/10.1021/acsomega.1c01072
ACS Omega 2021, 6, 14298−14308

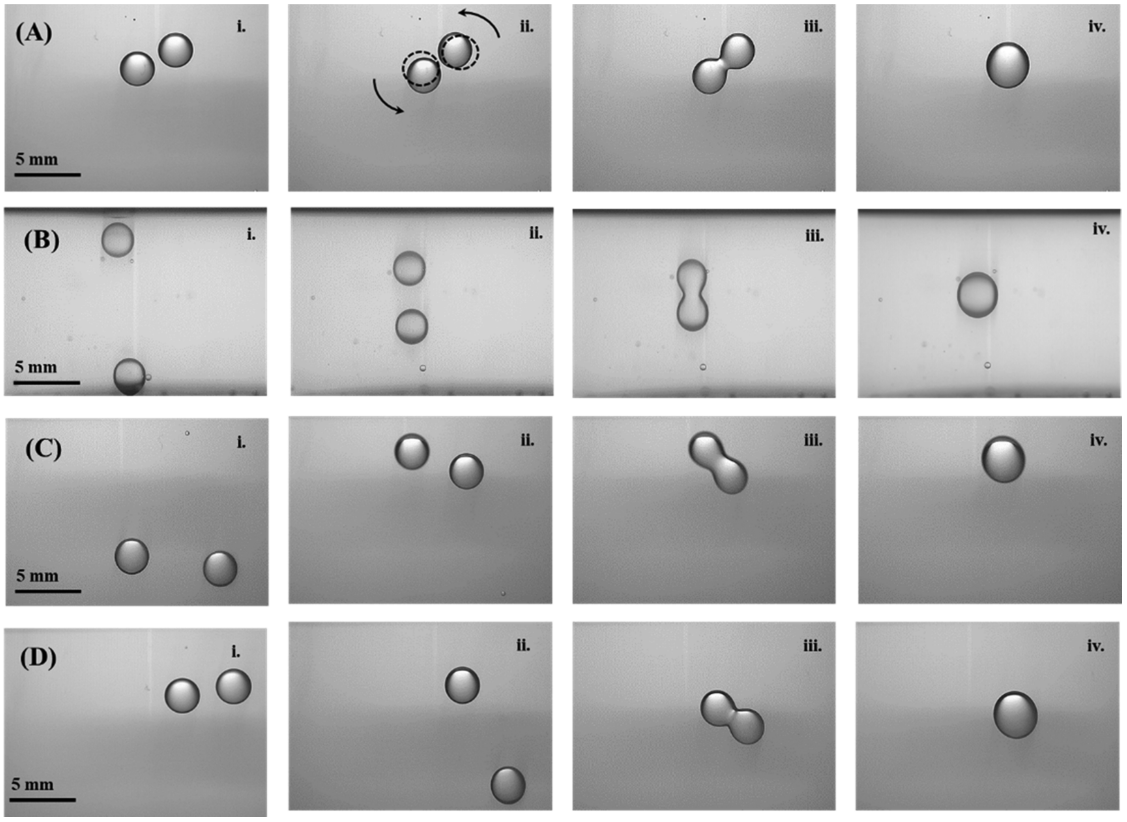

Figure 2. Impact of DDI, migratory coalescence, and DEP force on the coalescence of two water droplets in an oil medium. Two 10 μL deionized water droplets were dispersed in four different positions/orientations (A–D) inside a test cell containing silicone (oil 3000 cSt viscous). In (A), the distance between the water droplets was close enough to activate the DDI mechanism immediately. In this case, the tangential (angular) component (eq S2) caused the rotation of the dipoles; then, the radial component (eq S1) reached the positive value and coalesced. In (B), the two water droplets were in the center and far from each other, and the DDI had a small effect on attracting water droplets. The upper water droplet first acquired charges from the surface of the dielectric and the lower water droplet acquired charges from ground electrode. They are both moved toward the opposite electrode due to the effect of EP. The lower water droplet was polarized. The charge induced on the top surface did not agree in sign with the moving droplet, which caused attraction in the neighboring region and coalesced after the collision. (C, D) None of the above mechanisms were activated in the first place, and droplets started bouncing between the two electrodes because of EP, but as an effect of DEP, they moved to the center of the test cell and coalesced.

opposite electrodes (Figure 2B). Water droplets touching any electrode surface receive a free charge, which is given by eq S3.

However, it is to be noted that the amount of charges varies from point to point on the oil surface and depends on the surface potential, as described in eq 4. Water droplets travel the gap between the electrodes to reach the opposite electrode due to Coulombic forces. Coalescence can occur in this gap due to the collision between the nearby water droplets or the attraction force between the neighboring oppositely charged water droplets. In the case of attraction, the force acting between the water droplets can be found from eq S5.

This force, responsible for electrocoalescence between two water droplets, is called migratory coalescence, which is EP in nature and usually occurs in DC electric fields (or AC electric fields with a low frequency). Migratory coalescence should be considered when the water droplets succeed in keeping their charge long enough to pass the gap or at least halfway, depending on the relaxation time. In this experiment, the relaxation time (400 s) is high enough to guarantee water droplets traversing the gap between the electrodes and experiencing the migratory coalescence. According to eq S3 and comparing with eq S1, it can be concluded that migratory coalescence is significantly affected by the size of water droplets rather than their distance; however, the DDI is mostly affected and manipulated by the distance between the water droplets rather than their sizes. On the other hand, with an increase in the strength of the electric field, both forces increase in 2-folds in the migratory coalescence and the DDI phenomena. Consequently, the opposite charges were induced in the water droplets. They started to migrate from one electrode to another one; however, the signs of the charges do not agree, and the droplets attract each other and merge due to the coalescence process based on eq S5. Although the duration of the whole event was 20 s and it was higher than that observed time in the DDI process, it could be considered a fast response since the distance between the water droplets (see Video S3) is relatively larger than that of the previous case.

Both DDI and migratory coalescence have been observed under a uniform electric field. When water droplets are very far, the uniform electric field is not efficient in enabling electrocoalescence. However, a nonuniform electric field forms while utilizing the corona discharge and the droplets exhibit different behavior. To examine this, another experiment was conducted. One water droplet was dispersed in the center and another at the right of the test cell (oil medium), where the electric field is weaker (Figure 2C). In a conventional electrocoalescence where the electric field is uniform, there is no chance of coalescence of these two water droplets. Due to

https://doi.org/10.1021/acsomega.1c01072
ACS Omega 2021, 6, 14298−14308

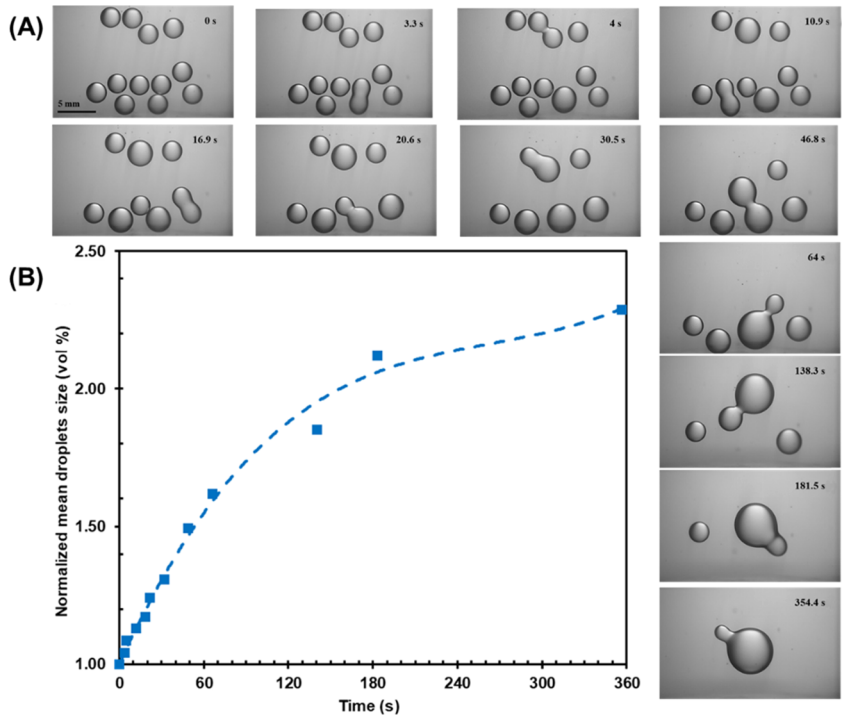

Figure 3. (A) Twelve 10 μL deionized water droplets were dispersed in the test cell. DDI showed a rapid response to the applied electric field (4 kV) and was responsible for all coalescence events in the first 20 s of treatment with corona discharge. The second mechanism of the coalescence was activated when the first water droplet touched the top surface of the dielectric. Subsequently, the migratory motion was the main reason for coalescence events, the so-called migratory coalescence. The DEP force increased the rate of coalescence by gathering the far-off water droplets in the center and is involved in coalescence events after 138 s of treatment. (B) Normalized mean droplet size (volume-weighted vs time). This plot shows a rate of coalescence, which decreases gradually over time, changing the mechanism of coalescence from DDI to migratory coalescence. Although the rate of coalescence is decreased in migratory coalescence, it is still a promising mechanism since the normalized water droplet size increased from 1.25 to 2.25.

the considerable distance between the droplets, neither DDI nor migratory coalescence can be activated. DEP could simply be translated as the motion of matter due to the polarization effect in a nonuniform electric field. Unlike EP that the movement in an electric field is dependent on charged particles, the motion in DEP results from the difference in the dielectric constant of materials in the electric field, the materials with the higher dielectric constant move toward stronger electric fields. Since the induced water droplet dipoles have a limited charge in an electric field, they align with the electric field lines. However, in a nonuniform electric field, one side of the dipoles is always exposed to the higher electric field rather than the other sides. In this case, the net force is not zero, and the dipole moves toward the regions with stronger electric fields. Also, it should be noted that the DEP force does not depend on the direction of the electric field and the dipole moves in the same direction even if the direction of the field is reversed and can be described by eq S6.

The nonuniform distribution of the electric field component described in eqs 4 and 5 can result in the nonzero value of the electric field gradient in the above equation. The DEP forces move the water droplets toward space with the stronger electric field in a collective way and increase the effect of the DDI and the EP. The DEP can significantly enhance the performance of coalescence, especially in dilute emulsions. Also, the DEP can still be seen in charged water droplets due to either partial charging when being in contact with the electrodes or discharging based on the oil relaxation time. At the beginning of this experiment, the water droplets were bouncing in the oil medium between its top surface and the ground electrode during the discharge exposure. This behavior, also known as a ping-pong motion, was found in some other applications in the literature but not in the coalescence field.[45] It is hypothesized that when the EP starts, it is the main force that manipulates the motion of the water droplets inside of the oil medium. The observed secondary force was DEP, the effect of which can be expressed as two components in the vertical and horizontal axes. With a nonuniform electric field induced via corona discharge, the field is stronger close to the surface in the vertical direction, and the direction of the DEP is upward. This observation confirms the electric field distribution that is expressed in eqs 4 and 5. The velocity of the water droplets in the upward direction was faster than that of the downward motion even though the gravity force agreed in that direction. Ultimately, the horizontal component of the DEP was responsible for the coalescence. The electric field became stronger by approaching the center of the test cell; therefore, the direction of the DEP was toward the center. The center droplet was already exposed to the strongest electric field, and it did not have any motion in the horizontal direction. The right-hand-side droplet was exposed to the weaker electric field, and exposure of the DEP force pushed it to the center of the test cell, decreasing the distance between the two droplets. This process increased the chance of collision, activating Coulomb's force between two droplets, as expressed in eq S5. Coalescence was initiated once the water droplets with opposite charges were sufficiently close to attracting each other due to the attraction force between two opposite charges,

https://doi.org/10.1021/acsomega.1c01072
ACS Omega 2021, 6, 14298−14308

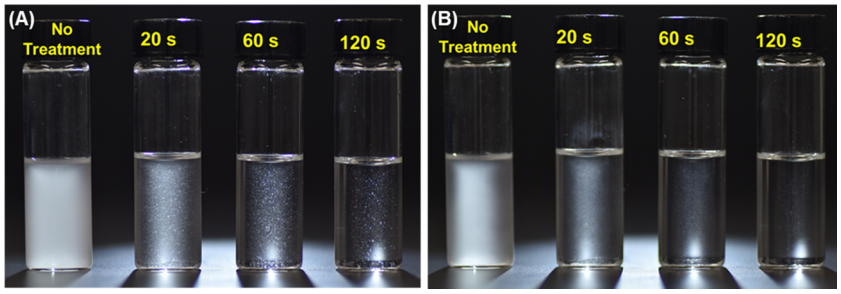

Figure 4. Effect of the corona discharge on the concentrated emulsion. (A) Effect of different corona treatment times (from left to right: no treatment, 20, 60, and 120 s of treatment, respectively) on the W/O emulsion (2% water content by weight in silicone oil with a viscosity of 350 cSt). The size of the water droplets gradually increased over the treatment time. (B) Samples from (A) after 24 h in shelf condition. Forming larger water droplets after corona treatment helps the separation of two phases by accelerating the sedimentation of the water droplets at the bottom of the vials. The sample with the highest treatment time (120 s) was nearly separated into two distinct phases.

leading to a collision between them. This process took 7 min 50 s to complete, which was dramatically longer than those observed in experiments described in Figure 2A,B. However, merging two distant droplets would not be possible if the electric field was uniform, which typically occurs in conventional electrocoalescence methods. This indicates the effectiveness of utilizing a nonuniform electric field for the coalescence of faraway droplets that is observed using a contactless corona discharge (see Video S4).

Finally, both water droplets were dispersed on the right side of the corona needle/test cell where the electric field is very weak (Figure 2D). Similar to what was observed in Figure 2C, water droplets exhibited bouncing between the two electrodes. The effect of the DEP was still observed, and the two water droplets started to move toward the center of the test cell. Coalescence was triggered when the distance between two water droplets was short enough to activate the migratory coalescence mechanism, leading to their attraction to each other. This event took 7 min 10 s, and it was relatively similar to that observed in Figure 2C, suggesting that the effect of the DEP on coalescence is independent of the distance between water droplets and only depends on the strength of the electric field, where the droplets are placed (see Video S5).

2.2. Coalescence of Multiple Water Droplets in an Oil Medium. To investigate the effect of corona discharge on the coalescence of more droplets collectively and to confirm previously observed phenomena, 12 droplets of deionized water (10 μL each in volume) were dispersed randomly in the cell and were exposed to a corona discharge induced by a 4 kV applied voltage (Figure 3A). As corona discharge initiates, DDI starts to dominate all of the coalescence events in the first 20 s (see Video S6). This force affected all of the adjacent water droplets leading to the formation of larger droplets. Beyond this time, by forming larger droplets, the distance between the water droplets increased and the rating of the DDI-induced coalescence decreased. After 10.9 s, the larger water droplets on the top touched the surface, receiving a positive charge, and started moving toward the ground electrode. From this point, migratory coalescence started to become the dominant mechanism for the rest of the process. The formation of the larger water droplets after 46.8 s enhanced de-emulsification since the small water droplets could easily suck into the interface of the larger droplet. The last water droplet, which also was the far-off water droplet from the center, merged nearly after 6 min as the effect of both EP and DEP.

Figure 3B shows the normalized mean droplet volume defined as the ratio of the average water droplet diameter (volume-weighted) to its initial diameter (~2.67 mm) vs time for the first 360 s after applying corona discharge. This graph can be divided into two sections: the first 20 s, which was dominated by the effect of DDI, and it can be considered relatively fast, and the second part from 20 s to the complete coalescence, which was dominated by migratory coalescence and the DEP-induced movement. The second part is quite slow due to the distance between water droplets, but the effect of the DEP is promising for the complete coalescence of all droplets and enhancing the overall performance. In addition, it should be noted here that the DEP helps to form larger droplets in the center, which can enhance the performance of the coalescence by sucking the smaller water droplets in the affected neighboring regions. Overall, the results obtained observing multiple droplets confirm the findings of two droplet coalescence and suggest the effectiveness of applying a nonuniform electric field via corona discharge on the separation of emulsions.

2.3. Coalescence of Many Water Droplets in Water/Oil Emulsion. To investigate the effect of the corona discharge on a real emulsion, a W/O emulsion (2% water content by weight in 350 cSt viscous silicone oil) was prepared and then transferred to a cell in three batches and was exposed to a 7 kV corona discharge for 20, 60, and 120 s. An applied voltage of 7 kV was selected to ensure that the surface potential is above the critical voltage, enabling observation of the electroconvection phenomenon and its effect against potential chain formation. One sample without treatment was kept as a control sample. Figure 4A shows the effect of different treatment times on the size of the water droplets. The size of the water droplets significantly reacted to the treatment time in which the larger droplets corresponded to more corona treatment time. It is evident that only 20 s of corona treatment leads to considerable coalescence of water droplets in the emulsion. Figure 4B shows the same samples (both treated and untreated) after 24 h in shelf conditions (see Video S7). The untreated emulsion appears to be milky without a considerable sign of separation even after 24 h. However, the treated emulsions continue to separate further even after the corona discharge; this is despite having smaller-sized water droplets when compared to the untreated emulsion. We believe that the induced charges in the emulsion due to the corona discharge are contributing to shelf-condition separation and sedimentation of the water droplets, significantly beyond what could be achieved without any treatment. Also, the effect of the residual charges in the mixture is negligible since comparing the control sample with the samples treated for different times does not

https://doi.org/10.1021/acsomega.1c01072
ACS Omega 2021, 6, 14298−14308

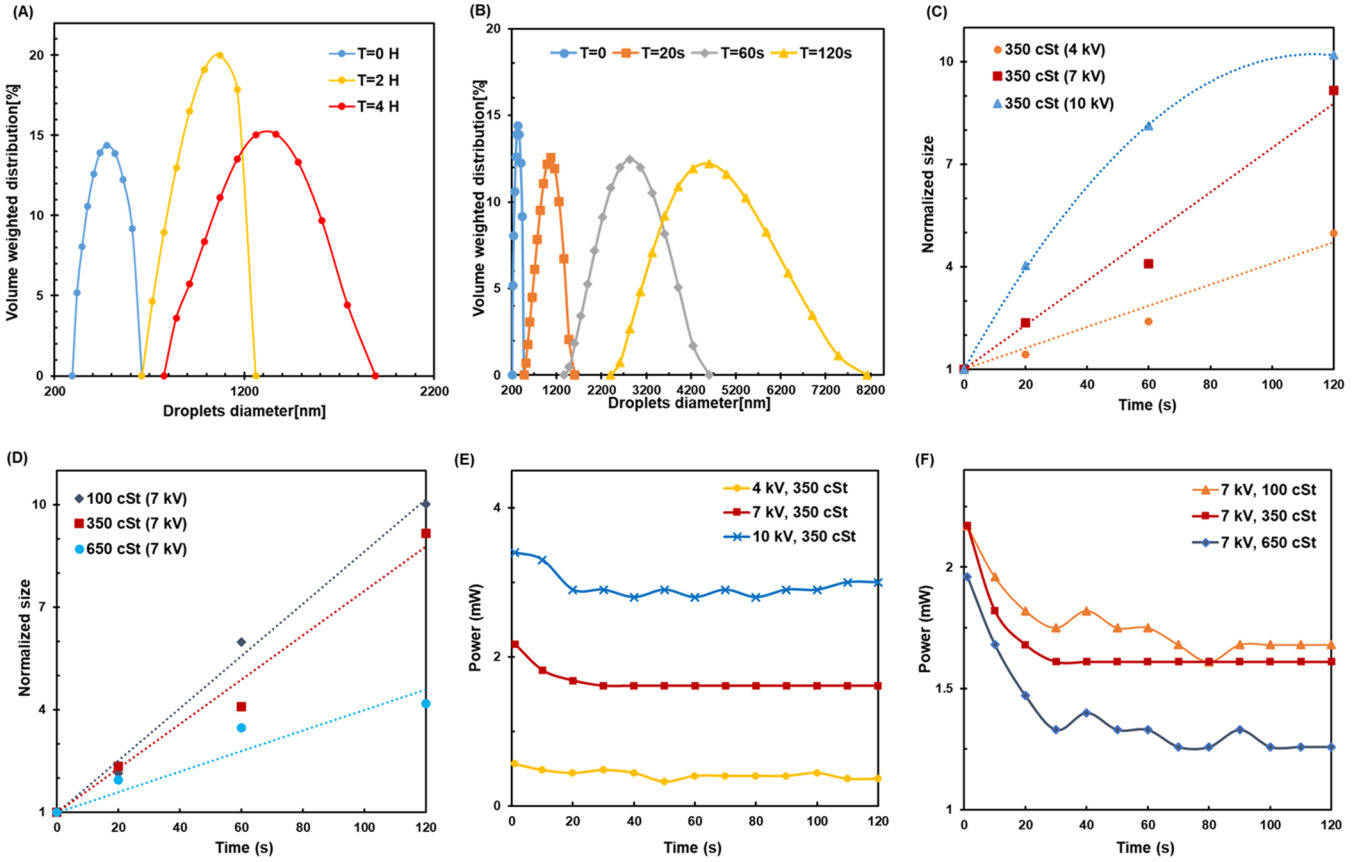

Figure 5. Effect of corona discharge on the diluted emulsion. (A) Changing in the droplet size distribution of diluted emulsion, including silicone oil with 100 cSt viscosity vs time without corona treatment over 4 h. The peak volumes were ∼460.8, 972.6, and 1266.7 nm for T = 0, 2, and 4 h, respectively. (B) Changing in the droplet size distribution of diluted emulsion including silicone oil with 100 cSt viscosity vs time. The peak volume-weighted sizes were ∼460.8, 989.3, 2756.8, and 4619.6 nm for T = 0, 20, 60, and 120 s, respectively (exposed to a 7 kV corona discharge). The size gradually shifts to larger sizes without tiny residual droplets. (C) Normalized water droplet size against corona treatment time in diluted emulsion (350 cSt) for different applied voltages. The higher voltage corresponds to the faster coalescence rate. The polynomial curve suggests a transition from DDI to migratory coalescence mechanisms using 10 kV voltage. (D) Effect of the different oil viscosities on the coalescence rate. Lower viscosity resulted in a faster rate with the same treatment conditions. (E) Power consumption of the case (C); the consumed power increases nonlinearly by increasing the voltage with a jump from 4 to 7 kV applied voltage. (F) Effect of viscosity on power consumption; less viscosity of continuous phase (oil) corresponds to higher power consumption, suggesting the electroconvection effect.

show any sign of stability on all of the treated samples after 24 h. Furthermore, using the higher voltage causes the motion inside of the oil inside the test cell, which was symmetrical on both sides vs the location of the corona needle (tip). The movement of the charged droplets made a flow pattern in the center from the ground electrode toward the surface (positive electrode). This motion can be amplified as a result of the ionic wind on the oil surface.[36,43] Initiating such a motion can also enhance the performance of the coalescence due to increasing the chance of collision between the water droplets[46] and preventing/breaking chain formation inside the emulsion (see Video S8).

2.4. Diluted Emulsion. The average distance between the water droplets in a diluted emulsion is relatively higher when compared to the size of the droplets. As a result, water droplets cannot build up enough interaction energy to attract each other. In addition, the existing nanodroplets in the emulsion make the separation process even more problematic because of the lower electrical forces and the lower sedimentation times. Experiments were carried out to evaluate the effect of corona discharge on emulsion with less than 0.1% water content by weight. Four treatment times (0, 20, 60, and 120 s), three applied voltages (4, 7, and 10 kV), and three different viscosities of silicone oil (100, 350, and 650 cSt) were studied, evaluating the effect of these parameters on the coalescence rate. The initial size distribution at the beginning of the test was considered as a baseline for a comparative evaluation purpose. The natural coalescence of the emulsions has a limited response on time, and the size distribution slowly shifted to a larger size over 4 h (see Figure 5A). When the emulsion of silicone oil (100 cSt viscous) was exposed to a 7 kV corona discharge, the volume-weighted size distribution showed a rapid response to the corona treatment. Not only the average size was shifted but also tiny water droplets in the scale of nano coalesced and formed larger droplets in the scale of macro, without leaving residual droplets (see Figure 5B). Figure 5C shows the effect of the electric field strength on the rate of coalescence. The water droplet sizes immediately responded to the applied electric field, and the size of water droplets increased over time. The highest electric field corresponds to a higher coalescence rate. At the highest applied electric field (10 kV) and after 60 s of treatment, the rate of the coalescence decreased and then it reached the limit range of the dynamic light scattering (DLS) size, above which the size of the droplets cannot be measured by this method. The curve no longer follows the linear trend observed in other

https://doi.org/10.1021/acsomega.1c01072
ACS Omega 2021, 6, 14298−14308

experiments and seems to be polynomial. These findings agree with the quantitative analysis results shown in Figure 4B, suggesting that the initial rapid response was due to the DDI and the slower response was due to the DEP and migratory coalescence.

The results were also compared with conventional electrocoalescence via a uniform electric field in the literature. As an instance, Williams et al.[26] used a 4 kV voltage and formed a uniform electric field to separate 0.1% W/O emulsion with a silicone oil viscosity of 1 cSt. They observed electrocoalescence via enlargement of water droplets reaching a diameter of ∼1.6 normalized sizes (after 30 s) and saturating afterward without any further increase in size. Here, we used a much viscous silicone oil (350 cSt vs 1 cSt) and showed continuous and more rapid coalescence verified by an increasing trend in the size of the water droplets as a function of processing time. We observed water droplets reaching 1.6 normalized sizes only after 20 s of treatment and continuously enlarging to 5 normalized sizes after 120 s, without any sign of saturation in coalescence trend/behavior. This continuous coalescence of water droplets in the diluted emulsion is due to the presence of the DEP forces formed by the nonuniform electric field induced via corona discharge. The DEP forces decrease the distance between the water droplets by bringing them to the center of the test cell, leading to an overall enhancement in the coalescence/separation process. It is to be noted that this improved coalescence behavior occurred while the viscosity of our silicone oil (350 cSt) is significantly higher than that reported by Williams et al. (1 cSt). This is notable considering higher drag forces and resistance to motion of water droplets when aiming to move in more viscous oil media. The experiment conducted on emulsions with various viscosity oils exhibited the volume distribution normalized to the initial value (Figure 5E). In all cases, shifting to larger water droplets was observed; however, by increasing the viscosity, the rate of the coalescence decreased as expected due to the hydrodynamic drag force and damping force exerted by the squeezed fluid film (i.e., oil layer) between the approaching droplets.[3] A small decrease in the coalescence rate was observed when oil viscosity in the emulsion increased more than 3 times (from 100 to 350 cSt). This suggests the dominant effect of the electric forces overcoming hydrodynamic forces that are induced by viscosity.

After 120 s of treatment under a 7 kV applied voltage, the size of the water droplets reached the same size as the emulsion treated under 10 kV, although no rapid increase in water droplet size was observed (Figure 5C). Figure 5E shows the electrical power consumption during the discharge. The power was calculated based on the measuring current and applied voltage over time ($P = V{\cdot}I$). The consumed power with a 10 kV applied voltage is nearly 2 times the one experienced with the 7 kV voltage, suggesting an optimum operating condition for efficient electrocoalescence and less power consumption using corona discharge. The oil with higher viscosity consumed less power compared to that with a lower viscosity due to the lower convective flow inside the emulsion with more viscous oil (see Figure 5F). In other words, increasing the voltage resulted in increasing the coalescence rate in the emulsion to a point in which the convection motion increases without increasing the coalescence rate. This undesired convection motion causes more power consumption and poor electrocoalescence performance. This behavior needs to be considered in search of the best recipe for separating emulsions with different oil viscosity values and overweighed against chain inhibitor behavior.

3. CONCLUSIONS

A contactless method of emulsion destabilization is presented utilizing a corona discharge that induces a nonuniform electric field in the emulsion. First, a qualitative analysis was conducted via monitoring coalescence patterns of multiple macrosized water droplets (diameter of ∼2.67 mm) inside an oil medium captured using a high-speed camera. We found that dipole−dipole interaction (DDI), migratory coalescence, and dielectrophoresis (DEP) are three major phenomena that induce the coalescence of water droplets. While DDI is playing a major role in the initial attraction of water droplets, the migratory coalescence is enabling the collision or attraction of oppositely charged water droplets. However, the DEP is increasing the coalescence rate by bringing the water droplets to the center due to the nonuniform electric field that is created by the corona discharge as a key feature of our separation approach. Next, a quantitative analysis was performed to study the impact of corona discharge on the coalescence of water droplets in micro/nanoemulsions using dynamic light scattering (DLS) measurements. We showed that increasing the input voltage and lowering the oil viscosity result in a faster coalescence rate, while power consumption increases nonlinearly by an increase in the input voltage. Finally, we found an optimum operating condition for power-efficient electrocoalescence and separation, utilizing the corona discharge. This suggests that our method can be tailored for efficient separation of emulsions with given oil properties.

Some common separation methods such as centrifugation and membrane separation are not energy-efficient and/or environmentally friendly and are incapable of separating a wide range of oil and water emulsions while often involving installation and operation complexities.[7−11,15] The contactless nature of our separation has several advantages over current methods used in industries. Simplicity in setting up and starting the process and minimal need for maintenance make our approach a reliable alternative for remote and offsite applications where mobility, flexibility, and time efficiency are needed. Unlike traditional electrocoalescence, the anode (sharp conductive needle) in a positive corona discharge is contactless (not connected directly to the emulsion) and consequently does not experience electrolytic corrosion. Besides, the air gap between the needle and the liquid (W/O mixture or emulsion) acts as a dynamic overcurrent resistor to protect the electrocoalescer against short circuits due to bridge formation between water droplets. The corona discharge is a room-temperature process (cold discharge); however, for extra safety in contained working conditions, nitrogen or other inert gases could be used to create ions and separate water from oil. The risk of attaching water droplets to an electrode and forming tiny droplets due to cone formation is also decreased since the number of wetted electrodes is reduced to one (just cathode electrode is in contact with the medium).

In the future, our contactless electrocoalescence method can be scaled up for bulk separation of high-volume emulsions by designing and adapting a wire and/or a grid electrode configuration. In addition, further study could focus on the electrocoalescence of nanoemulsions stabilized using surfactants. Besides, it is recommended for future works to form corona discharge in inert gases (i.e., nitrogen or argon) instead

https://doi.org/10.1021/acsomega.1c01072
ACS Omega 2021, 6, 14298−14308

of air and study their impact on oil/water separation using the geometry of multiple electrodes.

4. MATERIALS AND METHODS

A high-speed camera (Olympus TR i-speed) capable of up to 10 000 fps combined with a macrophotography lens (Tamron 90 mm 1:2.8) was used to capture the side videos and images (at 10 fps for droplets and 30 fps for emulsion experiments). The high-voltage amplifier (TREK Model 10/10B-HS) was connected to a DC power supply (BK 1698), which was used as a reference to the high-voltage amplifier. The amplifier can generate high-voltage DC (both positive and negative) and AC by a 1:1000 ratio. In these experiments, the positive DC was only used to generate corona discharge to avoid direct contact of the anode to emulsions and protect the electrode against corrosion. Figure S3A,B shows a tungsten needle before and after 100 h of corona discharge service under a high-resolution optical microscope without any sign of corrosion. The current was actively monitored by connecting the Keithley 2100 digital multimeter to the HV amplifier.

To understand the fundamentals of coalescence by the corona discharge, 10 μL water droplets (deionized water, Sigma-Aldrich, diameter of ~2.67 mm) were dispersed through a steel needle using a Ramé-Hart automated dispensing system (Model P/N 100-22) with an accuracy of $\pm$0.002 μL. The water droplets directly sunk into the large cubic quartz cell with the size of 30 × 30 × 30 mm^3 ($W \times D \times H$) and a 1 in. copper disk fixed to its bottom, acting as a grounding electrode. The test cell was then filled to 15 mm of height with 3000 cSt silicone oil (obtained from Hudy). The corona gap (t) was kept constant at 10 mm to assure that the ionic wind created by the corona discharge can reach all oil surfaces based on Warburg's law.

To examine the effectiveness of the corona discharge on emulsion separation, two types of W/O emulsions were prepared using different processes. The first type of emulsion consisted of the 2% water and a 98% silicone oil (350 cSt viscous obtained from MicroLubrol) content by weight agitated for 5 min by a magnetic stirrer at 2000 rpm, followed by 5 min of mixing with a homogenizer (Waverly model H-100) at 4000 rpm. Then, the emulsion was transferred to a transparent plexiglass cell with the size of 25 × 10 × 30 mm^3 ($W \times D \times H$). The homogenizer rpm and the mixing time were experimentally obtained in a way that enables us to have a proper droplet size range for optical observation of the electroconvection, chain formation, coalescence, and sedimentation using a regular camera. In the second type of emulsion, the preweighted water and oil (less than 0.1 wt % water in oil) were mixed in a beaker by a magnetic stirrer (BIPEE model SH-2) at 2000 rpm for 5 min at room temperature (temperature = 25 °C for both emulsions), followed by a final mixing by the homogenizer at 6000 rpm for 20 min. After that, the emulsions were transferred into a customized size 20 × 20 × 30 mm^3 ($W \times D \times H$) plexiglass cell and exposed to corona discharge. The sample preparation process was experimentally set in a way that emulsions with a small and uniform dispersion of water droplets suitable for the DLS measurements were obtained repeatedly. The dielectric media in these experiments were silicone oils with three different viscosities of 100, 350, and 650 cSt (obtained from MicroLubrol and XTR). The oil conductivities were measured with a rudimentary setup using standard 4 mm electrophoresis cuvettes as test cells. The conductivity of silicone oils with different viscosities was found to be ~6×10^{-12} S/m and close to that expected. For each set of experiments, these emulsions were made separately, following the same procedures mentioned above. Water droplet size distributions were quantified using the DLS instrument made by an Anton Paar model Litesizer-500 (measuring range: 0.3 nm to 10 μm particle diameter). The DLS determines the size of water droplets based on their refractive factor compared to the oil medium. Samples were uniformly extracted from all sides of each cell to ensure that the results represent real size distribution in each emulsion.

■ ASSOCIATED CONTENT

Supporting Information

The Supporting Information is available free of charge at https://pubs.acs.org/doi/10.1021/acsomega.1c01072.

Disintegration of a water droplet as the effect of charge accumulation in the tip of the water droplet (Video S1); DDI mechanism acting between two water droplets (2× faster playback) (Video S2); migratory coalescence mechanism acting between two water droplets (2× faster playback) (Video S3); migratory coalescence and DEP triggering coalescence event (32× faster playback) (Video S4); migratory coalescence and DEP triggering coalescence event (28× faster playback) (Video S5); coalescence of multiple droplets (variable speed) (Video S6); phase separation of W/O emulsion after corona treatment over 24 h (Video S7); and coalescence in concentrated emulsion (4× faster playback) (Video S8) (ZIP)

Experimental setup (Figure S1); interaction between two water droplets under a nonuniform electric field (Figure S2); and tungsten needle under an optical microscope (Figure S3) (PDF)

■ AUTHOR INFORMATION

Corresponding Author

Hossein Sojoudi − *Department of Mechanical, Industrial, and Manufacturing Engineering, The University of Toledo, Toledo, Ohio 43606, United States;* orcid.org/0000-0002-5278-9088; Email: hossein.sojoudi@utoledo.edu

Authors

Mohcen Shahbaznezhad − *Department of Electrical Engineering and Computer Science, The University of Toledo, Toledo, Ohio 43606, United States*

Amir Dehghanghadikolaei − *Department of Mechanical, Industrial, and Manufacturing Engineering, The University of Toledo, Toledo, Ohio 43606, United States*

Complete contact information is available at: https://pubs.acs.org/10.1021/acsomega.1c01072

Notes

The authors declare no competing financial interest.

■ REFERENCES

(1) Eow, J. S.; Ghadiri, M.; Sharif, A. O.; Williams, T. J. Electrostatic Enhancement of Coalescence of Water Droplets in Oil: A Review of the Current Understanding. *Chem. Eng. J.* **2001**, *84*, 173−192.

(2) Sadeghi, H. M.; Sadri, B.; Kazemi, M. A.; Jafari, M. Coalescence of Charged Droplets in Outer Fluids. *J. Colloid Interface Sci.* **2018**, *532*, 363−374.

(3) Mhatre, S.; Vivacqua, V.; Ghadiri, M.; Abdullah, A.; Al-Marri, M.; Hassanpour, A.; Hewakandamby, B.; Azzopardi, B.; Kermani, B. Electrostatic Phase Separation: A Review. *Chem. Eng. Res. Des.* **2015**, *96*, 177−195.
(4) Atten, P.; Raisin, J.; Reboud, J.-L. In *Field Induced Disruption of a Planar Water−Oil Interface Influenced by a Close Metallic Sphere*, IEEE International Conference on Dielectric Liquids, ICDL 2008, 2008; pp 1−4.
(5) Chiesa, M. In *Electrocoalescence Modeling: An Engineering Approach*, 15th Australasian Fluid Mechanics Conference, Sydney, Australia, 2004.
(6) Schramm, L. L. *Emulsions, Foams, and Suspensions: Fundamentals and Applications*; John Wiley & Sons, 2006.
(7) Klasson, K. T.; Taylor, P. A.; Walker, J. F.; Jones, S. A.; Cummins, R. L.; Richardson, S. A. Modification of a Centrifugal Separator for in-Well Oil-Water Separation. *Sep. Sci. Technol.* **2005**, *40*, 453−462.
(8) Chan, C.-C.; Chen, Y.-C. Demulsification of W/O Emulsions by Microwave Radiation. *Sep. Sci. Technol.* **2002**, *37*, 3407−3420.
(9) Xu, B.; Kang, W.; Wang, X.; Meng, L. Influence of Water Content and Temperature on Stability of W/O Crude Oil Emulsion. *Pet. Sci. Technol.* **2013**, *31*, 1099−1108.
(10) Sadek, S. E.; Hendricks, C. D. Electrical Coalescence of Water Droplets in Low-Conductivity Oils. *Ind. Eng. Chem. Fundam.* **1974**, *13*, 139−142.
(11) Solomon, B. R.; Hyder, M. N.; Varanasi, K. K. Separating Oil-Water Nanoemulsions Using Flux-Enhanced Hierarchical Membranes. *Sci. Rep.* **2015**, *4*, No. 5504.
(12) Takahashi, Y.; Koizumi, N.; Kondo, Y. Active Demulsification of Photoresponsive Emulsions Using Cationic−Anionic Surfactant Mixtures. *Langmuir* **2016**, *32*, 683−688.
(13) Couck, S.; Van Assche, T. R. C.; Liu, Y.-Y.; Baron, G. V.; Van Der Voort, P.; Denayer, J. F. M. Adsorption and Separation of Small Hydrocarbons on the Flexible, Vanadium-Containing Mof, Comoc-2. *Langmuir* **2015**, *31*, 5063−5070.
(14) Chiba, A.; Oshima, A.; Akiyama, R. Confined Space Enables Spontaneous Liquid Separation by Molecular Size: Selective Absorption of Alkanes into a Polyolefin Cast Film. *Langmuir* **2019**, *35*, 17177−17184.
(15) Wu, J.; Xu, Y.; Dabros, T.; Hamza, H. Effect of Demulsifier Properties on Destabilization of Water-in-Oil Emulsion. *Energy Fuels* **2003**, *17*, 1554−1559.
(16) Hano, T.; Ohtake, T.; Takagi, K. Demulsification Kinetics of W/0 Emulsion in an Ac Electric Field. *J. Chem. Eng. Jpn.* **1988**, *21*, 345−351.
(17) Lesaint, C.; Glomm, W. R.; Lundgaard, L. E.; Sjöblom, J. Dehydration Efficiency of Ac Electrical Fields on Water-in-Model-Oil Emulsions. *Colloids Surf., A* **2009**, *352*, 63−69.
(18) Berg, G.; Lundgaard, L. E.; Abi-Chebel, N. Electrically Stressed Water Drops in Oil. *Chem. Eng. Process.: Process Intensif.* **2010**, *49*, 1229−1240.
(19) Suemar, P.; Fonseca, E. F.; Coutinho, R. C.; Machado, F.; Fontes, R.; Ferreira, L. C.; Lima, E. L.; Melo, P. A.; Pinto, J. C.; Nele, M. Quantitative Evaluation of the Efficiency of Water-in-Crude-Oil Emulsion Dehydration by Electrocoalescence in Pilot-Plant and Full-Scale Units. *Ind. Eng. Chem. Res.* **2012**, *51*, 13423−13437.
(20) Pearce, C. The Mechanism of the Resolution of Water-in-Oil Emulsions by Electrical Treatment. *Br. J. Appl. Phys.* **1954**, *5*, 136.
(21) Bezemer, C.; Croes, G. Motion of Water Droplets of an Emulsion in a Non-Uniform Field. *Br. J. Appl. Phys.* **1955**, *6*, 224.
(22) Leary, T.; Yeganeh, M.; Maldarelli, C. Microfluidic Study of the Electrocoalescence of Aqueous Droplets in Crude Oil. *ACS Omega* **2020**, *5*, 7348−7360.
(23) Mainier, F. B.; Pardal, J. M.; Leite, P. P. B.; dos Reis, M. F. Passivation of the Zinc Anode of a Crude Oil Vertical Separator Resulting in Corrosion. *J. Mater. Sci. Eng. B* **2016**, *6*, 63−67.
(24) Luo, S.; Schiffbauer, J.; Luo, T. Effect of Electric Field Non-Uniformity on Droplets Coalescence. *Phys. Chem. Chem. Phys.* **2016**, *18*, 29786−29796.
(25) Vivacqua, V.; Mhatre, S.; Ghadiri, M.; Abdullah, A.; Hassanpour, A.; Al-Marri, M.; Azzopardi, B.; Hewakandamby, B.; Kermani, B. Electrocoalescence of Water Drop Trains in Oil under Constant and Pulsatile Electric Fields. *Chem. Eng. Res. Des.* **2015**, *104*, 658−668.
(26) Williams, T. J.; Bailey, A. G. Changes in the Size Distribution of a Water-in-Oil Emulsion Due to Electric Field Induced Coalescence. *IEEE Trans. Ind. Appl.* **1986**, *3*, 536−541.
(27) Luo, X.; Yan, H.; Huang, X.; Yang, D.; Wang, J.; He, L. Breakup Characteristics of Aqueous Droplet with Surfactant in Oil under Direct Current Electric Field. *J. Colloid Interface Sci.* **2017**, *505*, 460−466.
(28) Atten, P. In *Electrohydrodynamics of Dispersed Drops of Conducting Liquid: From Drop Deformation and Interaction to Emulsion Evolution*, Proceedings of the International Symposium on Electrohydrodynamics, Gdansk, Poland, 2012.
(29) Ristenpart, W.; Bird, J.; Belmonte, A.; Dollar, F.; Stone, H. Non-Coalescence of Oppositely Charged Drops. *Nature* **2009**, *461*, 377.
(30) Mhatre, S.; Thaokar, R. Electrocoalescence in Non-Uniform Electric Fields: An Experimental Study. *Chem. Eng. Process.: Process Intensif.* **2015**, *96*, 28−38.
(31) Xu, J.; Li, B.; Sun, Z.; Wang, Z.; Liu, B.; Zhang, M. Effects of Electrode Geometry on Emulsion Dehydration Efficiency. *Colloids Surf., A* **2019**, *567*, 260−270.
(32) Eow, J. S.; Ghadiri, M. Drop−Drop Coalescence in an Electric Field: The Effects of Applied Electric Field and Electrode Geometry. *Colloids Surf., A* **2003**, *219*, 253−279.
(33) Abd Rahman, N.; Ibrahim, F.; Yafouz, B. Dielectrophoresis for Biomedical Sciences Applications: A Review. *Sensors* **2017**, *17*, No. 449.
(34) Chang, J.; Lawless, P. A.; Yamamoto, T. Corona Discharge Processes. *IEEE Trans. Plasma Sci.* **1991**, *19*, 1152−1166.
(35) Mahmoudi, S. R.; Adamiak, K.; Castle, G. P. Spreading of a Dielectric Droplet through an Interfacial Electric Pressure. *Proc. R. Soc. A* **2011**, *467*, 3257−3271.
(36) Mohamed, M. H.; Shahbaznezhad, M.; Dehghanghadikolaei, A.; Haque, M. A.; Sojoudi, H. Deformation of Bulk Dielectric Fluids under Corona-Initiated Charge Injection. *Exp. Fluids* **2020**, *61*, No. 116.
(37) Akishev, Y.; Goossens, O.; Callebaut, T.; Leys, C.; Napartovich, A.; Trushkin, N. The Influence of Electrode Geometry and Gas Flow on Corona-to-Glow and Glow-to-Spark Threshold Currents in Air. *J. Phys. D: Appl. Phys.* **2001**, *34*, 2875−2882.
(38) Schneider, J.; Watson, P. Electrohydrodynamic Stability of Space-Charge-Limited Currents in Dielectric Liquids. I. Theoretical Study. *Phys. Fluids* **1970**, *13*, 1948−1954.
(39) Hartmann, G. *Spectroscopie De La Décharge Couronne: Étude Des Mécanismes De Collisions Dans Le Dard (Streamer)*; Universite de Paris-Sud, 1977.
(40) Perez, A. T. In *Electrohydrodynamic Instabilities in Dielectric Liquids Induced by Corona Discharge*, IEEE 12th International Conference on Conduction and Breakdown in Dielectric Liquids, ICDL'96, 1996; pp 126−129.
(41) Warburg, E. *Handbuch Der Physik*; Springer: Berlin, 1927; Vol. *14*, pp 154−155.
(42) Ramos, A. *Electrokinetics and Electrohydrodynamics in Microsystems*; Springer Science & Business Media, 2011; Vol. *530*.
(43) Ohyama, R.; Kaneko, K. In *Optical Characterization of Steady Electrohydrodynamic Fluid Motion Induced by Surface Corona Discharge*, 1998 Annual Report − Conference on Electrical Insulation and Dielectric Phenomena, Volumes 1 and 2, 1998; pp 158−161.
(44) Shahbaznezhad, M.; Dehghanghadikolaei, A.; Sojoudi, H. Optimum Operating Frequency for Electrocoalescence Induced by Pulsed Corona Discharge. *ACS Omega* **2020**, *5*, 31000−31010.
(45) Shojaeian, M.; Hardt, S. Mass Transfer Via Femtoliter Droplets in Ping-Pong Mode. *Phys. Rev. Appl.* **2020**, *13*, No. 014015.

https://doi.org/10.1021/acsomega.1c01072
ACS Omega 2021, 6, 14298−14308

(46) Vasilkov, S.; Chirkov, V.; Stishkov, Y. K. Electrohydrodynamic Flow Caused by Field-Enhanced Dissociation Solely. *Phys. Fluids* **2017**, *29*, No. 063601.

https://doi.org/10.1021/acsomega.1c01072
ACS Omega 2021, 6, 14298−14308